Crystal Structures of Intermediates in the Dehalogenation of Haloalkanoates by L-2-Haloacid Dehalogenase

Ridder, Ivo S.; Rozeboom, Henriëtte J.; Kalk, Kor H.; Dijkstra, Bauke W.

Published in:
The Journal of Biological Chemistry

DOI:
10.1074/jbc.274.43.30672

THE JOURNAL OF BIOLOGICAL CHEMISTRY
Vol. 274, No. 43, Issue of October 22, pp. 30672–30678, 1999

Printed in U.S.A.

Crystal Structures of Intermediates in the Dehalogenation of Haloalkanoates by L-2-Haloacid Dehalogenase*

(Received for publication, June 18, 1999)

Ivo S. Ridder, Henriëtte J. Rozeboom, Kor H. Kalk, and Bauke W. Dijkstra‡

From the Laboratory of Biophysical Chemistry and BIOSON Research Institute, Department of Chemistry, University of Groningen, Nijenborgh 4, 9747 AG Groningen, The Netherlands

The L-2-haloacid dehalogenase from the 1,2-dichloroethane-degrading bacterium *Xanthobacter autotrophicus* GJ10 catalyzes the hydrolytic dehalogenation of small L-2-haloalkanoates to their corresponding D-2-hydroxyalkanoates, with inversion of the configuration at the C_2 atom. The structure of the apoenzyme at pH 8 was refined at 1.5-Å resolution. By lowering the pH, the catalytic activity of the enzyme was considerably reduced, allowing the crystal structure determination of the complexes with L-2-monochloropropionate and monochloroacetate at 1.7 and 2.1 Å resolution, respectively. Both complexes showed unambiguous electron density extending from the nucleophile Asp^8 to the C_2 atom of the dechlorinated substrates corresponding to a covalent enzyme-ester reaction intermediate. The halide ion that is cleaved off is found in line with the Asp^8 Oδ1–C_2 bond in a halide-stabilizing cradle made up of Arg^{39}, Asn^{115}, and Phe^{175}. In both complexes, the Asp^8 Oδ2 carbonyl oxygen atom interacts with Thr^{12}, Ser^{171}, and Asn^{173}, which possibly constitute the oxyanion hole in the hydrolysis of the ester bond. The carboxyl moiety of the substrate is held in position by interactions with Ser^{114}, Lys^{147}, and main chain NH groups. The L-2-monochloropropionate CH_3 group is located in a small pocket formed by side chain atoms of Lys^{147}, Asn^{173}, Phe^{175}, and Asp^{176}. The size and position of the pocket explain the stereospecificity and the limited substrate specificity of the enzyme. These crystallographic results demonstrate that the reaction of the enzyme proceeds via the formation of a covalent enzyme-ester intermediate at the nucleophile Asp^8.

L-2-Haloacid dehalogenase (L-DEX)[1] catalyzes the hydrolytic dehalogenation of L-2-haloalkanoates to the corresponding D-2-hydroxyalkanoates with inversion of the configuration at the C_2 atom. Several homologous L-DEXs have been found in various *Pseudomonas* species and in *Xanthobacter autotrophicus* GJ10, a bacterium that is able to degrade the xenobiotic compound 1,2-dichloroethane (1, 2). This halogenated hydrocarbon is industrially produced in large quantities and is applied as a solvent and as an intermediate in the production of plastics (3). Because microorganisms that contain dehalogenases can be used in a biotechnological approach to detoxify halogenated aliphatics (4), such enzymes are a fascinating target for research. In addition, the stereospecificity of L-DEXs could make them useful for the biosynthesis of chiral 2-hydroxyalkanoic acids. Furthermore, L-2-haloacid dehalogenase is the prototypical member of a large superfamily of hydrolases, the haloacid dehalogenase (HAD) superfamily identified by Koonin and coworkers (5, 6). Based on three conserved sequence motifs, the L-DEXs, epoxide hydrolases, P-type ATPases, and a variety of phosphatases are recognized as members of this superfamily. Detailed information on L-DEXs is of interest as the enzyme is the only member of the HAD superfamily that has been structurally characterized so far.

The x-ray structures of two L-2-haloacid dehalogenases have been reported, L-DEX YL from *Pseudomonas* sp. YL (Protein Data Bank code 1JUD (7)) and DhlB from *X. autotrophicus* GJ10 (Protein Data Bank code 1AQ6 (8)). The enzymes share a sequence identity of 40%, and their structures are closely related. Both enzymes have a mixed α/β core domain in a Rossmann fold with a four-helix bundle subdomain insertion. DhlB is somewhat larger, and the 21 extra residues form a two-helix excursion from the α/β core domain on the same side as the four-helix bundle. Together these helical domains provide a tight dimer interface and limit the substrate specificity of the *X. autotrophicus* enzyme to short substrates such as haloacetates and halopropionates (8, 9).

Comprehensive biochemical data have been obtained for the *Pseudomonas* enzyme (1, 10, 11).[2] Asp^8 was identified as the nucleophile in the first step of the enzymatic reaction, the formation of a covalent enzyme-ester intermediate. Furthermore, these studies revealed eight more charged and polar amino acids (Thr^{12}, Arg^{39}, Ser^{114}, Lys^{147}, Tyr^{153}, Ser^{171}, Asn^{173}, and Asp^{176}) that are involved in substrate binding and catalysis. Most of the catalytically critical residues are conserved in the HAD superfamily and they stand out from the main domain. The only exception is Arg^{39}, which is provided by the four-helix bundle domain. The x-ray structures enabled a detailed discussion of the role of these residues, and in particular useful information could be extracted from a model of a bound L-2-monochloropropionate (MCPA) substrate, which was based on the position of a formate ion in the active site of DhlB (8). The conserved serine residue in motif II, Ser^{114}, was pro-

* This work was supported by the Netherlands Foundation for Chemical Research (SON) with financial aid from the Netherlands Organization for Scientific Research (NWO). The costs of publication of this article were defrayed in part by the payment of page charges. This article must therefore be hereby marked "*advertisement*" in accordance with 18 U.S.C. Section 1734 solely to indicate this fact.

The atomic coordinates and structure factors (codes 1qq5, 1qq7, and 1qq6) have been deposited in the Protein Data Bank, Research Collaboratory for Structural Bioinformatics, Rutgers University, New Brunswick, NJ (http://www.rcsb.org/).

‡ To whom correspondence should be addressed: Laboratory of Biophysical Chemistry, Dept. of Chemistry, University of Groningen, Nijenborgh 4, 9747 AG Groningen, The Netherlands. Tel.: 31-503634378; Fax: 31-503634800; E-mail: b.w.dijkstra@chem.rug.nl.

[1] The abbreviations used are: L-DEX, L-2-haloacid dehalogenase; L-DEX YL, L-2-haloacid dehalogenase from *Pseudomonas* sp. YL; DhlB, L-2-haloacid dehalogenase from *X. autotrophicus* GJ10; MCPA, 2-monochloropropionate; bis-Tris, bis(2-hydroxyethyl)iminotris(hydroxymethyl)methane; MCAA, monochloroacetate; r.m.s., root mean square; DhlA, haloalkane dehalogenase from *X. autotrophicus* GJ10.

[2] The residue numbering of the L-DEX YL enzyme is slightly different from that of DhlB. For clarity, homologous residues are numbered according to the DhlB sequence.

posed to bind the carboxylate moiety of the substrate, and a halide-binding cradle formed by Arg^{39}, Tyr^{10}, and Phe^{175} was postulated. Conserved residues from motifs I and III, Thr^{12}, Ser^{171}, and Asn^{173}, were found to interact with the nucleophile Asp^{8} Oδ2 atom possibly making up an oxyanion hole, and the motif III Lys^{147} Nζ was hydrogen-bonded to the Oδ1 atom of the nucleophile.

These proposals were recently corroborated by crystal structures of an inactive S171A L-DEX YL mutant enzyme covalently bound to several chloroalkanoate substrates (12, 13). However, structural evidence for the location of the halide ion is still lacking. To gain more insight into the abstraction of the halide ion and the reaction of the enzyme with MCPA, one of its best substrates (9), we extended our crystallographic studies on DhlB. One soaking experiment with MCPA was done at pH 8, at which the enzyme is active, to obtain information about the enzyme structure during or after processing of the substrate. Two other experiments were performed at low pH to trap the reaction intermediates of MCAA and L-MCPA in a similar way as was done previously for haloalkane dehalogenase (14). Here we present the 1.52 Å resolution structure of the unliganded enzyme and the structures of covalent ester intermediates of the native enzyme with L-MCPA and MCAA, including a bound chloride ion. The structures experimentally confirm the substrate binding model proposed earlier (8) and contribute to the detailed understanding of the reaction mechanism of the enzyme.

MATERIALS AND METHODS

Crystal Preparation—Crystals of L-2-haloacid dehalogenase were grown in the presence of sodium formate by macroseeding as described previously (15). The enzyme crystallizes in two orthorhombic space groups, $C222_1$ and $P2_12_12_1$. For the soaking experiment the better diffracting primitive crystal form was chosen (a = 56.75 Å, b = 83.83 Å, c = 90.81 Å, 2 mol/asymmetric unit). As formate binds in the active site of the enzyme, crystals were washed two times in fresh synthetic mother liquor (25% (w/v) polyethylene glycol 8000, 100 mM bis-Tris, pH 7.0) in an attempt to remove the formate.

One crystal was transferred to a solution of slightly higher pH, containing 25% (w/v) polyethylene glycol 8000, 100 mM bis-Tris, pH 8.0, equilibrated for 20 min at room temperature, and finally soaked for 3 h in synthetic mother liquor, pH 8.0, containing 20 mM D,L-2-monochloropropionic acid.

A second crystal was transferred to a more acidic solution of 25% (w/v) polyethylene glycol 8000, 100 mM citrate, pH 5.0, at 4 °C, equilibrated for 20 min, and soaked for 45 min at 4 °C in synthetic mother liquor containing 20 mM D,L-MCPA. A third, analogous experiment was done at pH 5.0 using 10 mM monochloroacetic acid (MCAA) instead of MCPA.

Diffraction Data Collection—Diffraction data were collected at cryotemperature (100 K) from single crystals at experimental station ID14-3, European Synchrotron Radiation Facility (ESRF), Grenoble (MCPA, pH 8 experiment) and at the European Molecular Biology Laboratory Outstation at Deutches Electronen Synchrotron, Hamburg, beamline X11 (MCPA, pH 5 experiment) and beamline X31 (MCAA, pH 5 experiment). The ID14-3 beamline (λ = 0.9475 Å) was equipped with a MarCCD detector system, and the X11 (λ = 0.9095 Å) and X31 (λ = 1.00 Å) beamlines with a 30-cm and a 18-cm MAR image plate area detector, respectively. Data were integrated and merged with DENZO/SCALEPACK (16). Data processing statistics are given in Table I.

Refinement of the pH 8 Structure—For the MCPA pH 8 experiment, the native DhlB structure (Protein Data Bank entry 1AQ6 (8)) without the formate ions and water molecules was positioned in the cell using AMoRe (17). Initial σ_A-weighted OMIT $2F_o - F_c$ and $F_o - F_c$ electron density maps (18–20) clearly showed density for a formate ion in the active site of both molecules, indicating that the substrate had not bound. Nevertheless, the model was refined because of the improved resolution compared with the 1AQ6 structure. The set of reflections set apart to calculate R_{free} values (21) in the refinement of the 1.95 Å native structure was extended to cover 5% of the additional data as well. After an initial round of rigid body refinement, the model was subjected to one refinement cycle of torsion-angle dynamics (22) and subsequent cycles of positional and B-factor refinement for all atoms and refinement of the occupancy of residues with two conformations, all performed with CNS 0.5 (23). Geometry checks pointed out a considerable number of N–Cα–C bond angles that deviated from their ideal value (24). Hence, the CNS topology and parameter files were adjusted such that the restraint on the main chain ω dihedral angle was relaxed to 20% of its original value without changing the restraints on the other X-N-C-X dihedral angles (X = any atom). This was done to allow for the large variability of the ω angle observed in atomic resolution structures (25, 26). After the adjustment, no deviating bond angles were flagged anymore. However, the ω angle of the nucleophile Asp^{8} became 163°, which is far off the normal value for a *trans*-peptide bond.

At all stages σ_A-weighted $2F_o - F_c$ electron density maps were calculated and inspected with O (27) to check the agreement of the model with the data. PROCHECK (28) and WHATCHECK (29) were used to assess the stereochemical quality. Whenever necessary the model was manually adjusted in O. When the refinement gave no further decrease in R_{free} nor any improvement in stereochemistry, it was considered completed. A final round of refinement including all data resulted in an overall crystallographic R-factor of 19.8% for data ranging from 20.0 to 1.52 Å resolution. Refinement and model statistics are given in Table I, and the quality of the electron density can be judged from Fig. 1*A*.

The asymmetric unit contains two protein molecules of residues 1–245 forming the DhlB dimer, 571 water molecules, and two formate ions. In molecule A, Arg^{25}, Glu^{79}, Thr^{93}, Lys^{109}, Gln^{122}, Ser^{172}, Ser^{186}, Met^{218}, Thr^{222}, and Glu^{225} have two conformations, and in molecule B, a second side chain position is found for Asp^{21}, Glu^{79}, Thr^{93}, Ser^{152}, Ser^{172}, Met^{218}, and Thr^{222}. In both molecules, the loop formed by residues 204–207 and the C termini have been remodeled, and in molecule B, the *cis*-peptide bond between Ala^{106} and Pro^{107} has been replaced by a *trans*-peptide bond. Furthermore, in both molecules the helix and loop formed by residues 122–132 have shifted by 0.6 Å on average, although no structural reason is apparent.

Refinement of the pH 5 Structure with MCPA Bound—For the MCPA pH 5 experiment, the 1.52 Å pH 8 structure described above was used as a starting model. Initial σ_A-weighted $2F_o - F_c$ and $F_o - F_c$ electron density maps clearly showed density extending from Asp^{8} Oδ1 for all MCPA atoms except for the chlorine, indicating that the substrate had bound covalently and that the chlorine atom had been cleaved off. The same refinement strategy as described above was employed. Unambiguous difference electron density enabled us to build in the covalently bound substrate (Fig. 1*B*). Also a chloride ion was identified in the active site on the basis of residual positive difference density around a "water molecule" with a B-factor of 2.0 $Å^2$ and the chemical environment. In addition, a diffraction experiment with a 2-monoiodoacetic acid substrate gave a peak of more than double intensity in the electron density map at this position (data not shown). Topology and parameter files for the covalently modified residue were generated with XPLO2D (30). At the end of the refinement, a final round including all data resulted in an overall crystallographic R-factor of 17.0% for data ranging from 20.0 to 1.70 Å resolution. Refinement and model statistics are given in Table I.

The DhlB structures with and without bound MCPA are very alike with an r.m.s. deviation of 0.24 Å for all Cα atoms of the dimer, so it can be concluded that the overall structure of the enzyme is not influenced by the binding of its substrate. The disorder observed with the pH 8 experiment in the loop that contains residues 25–27 (see "Results" and "Discussion") could be resolved in the B molecule in the MCPA experiment as two different conformations of the main chain in this region. In molecule A, Arg^{25}, Thr^{93}, Lys^{109}, Ser^{152}, Ser^{172}, Ser^{186}, Met^{218}, Thr^{222}, and Glu^{225} have two conformations, and in molecule B, a second side chain position is found for Lys^{41}, Arg^{54}, Glu^{79}, Thr^{93}, Gln^{100}, Lys^{109}, Ser^{152}, Ser^{172}, Ser^{186}, Met^{218}, and Thr^{222}. The region from residues Ala^{208} to Phe^{213} is disordered as was observed in the native enzyme, pH 8 (see "Results" and "Discussion"). In the refinement of the MCAA model these characteristics were preserved.

Refinement of the pH 5 Structure with MCAA Bound—For the MCAA pH 5 experiment, the pH 5 DhlB structure with the covalent MCPA intermediate bound was used as a starting model. An initial σ_A-weighted $2F_o - F_c$ electron density map clearly showed density extending from Asp^{8} Oδ1, and in the $F_o - F_c$ map negative electron density was observed at the C_3 position of the MCPA, indicating that the smaller MCAA substrate had bound. The chloride ion was also found in an analogous position. A similar refinement strategy as described above for the MCPA structure was employed. Residues with alternative conformations were preserved and their occupancies were not refined. Refinement was completed with a final round including all data, resulting in an overall crystallographic R-factor of 17.1% for data ranging

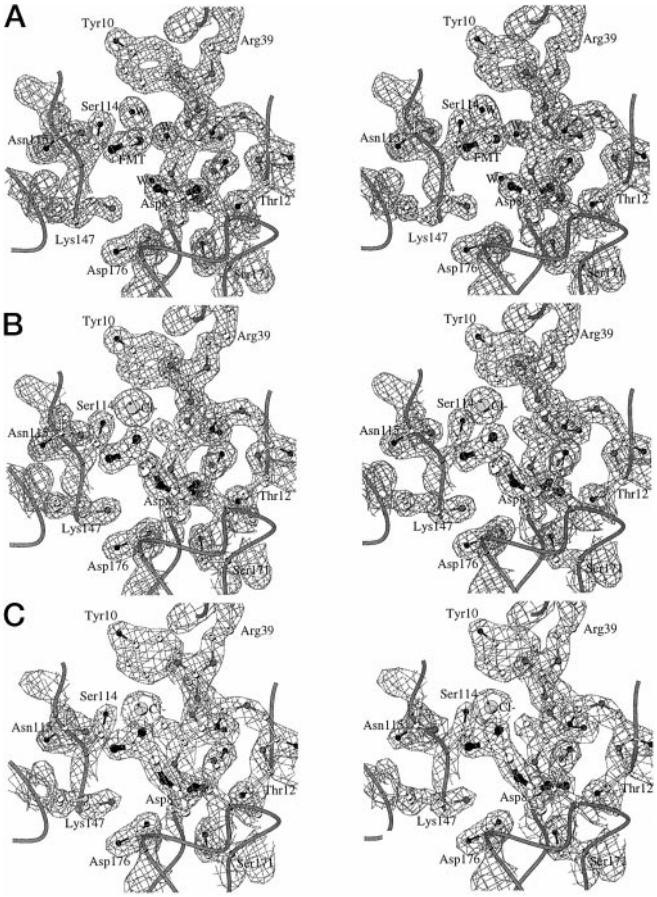

FIG. 1. **Stereo view of the active site of L-2-haloacid dehalogenase displayed with final $2F_o - F_c$ electron density.** *A*, 1.52 Å resolution structure with formate ion bound; *B*, structure with dechlorinated MCPA moiety covalently attached to Asp^8; *C*, structure with dechlorinated MCAA moiety covalently attached to Asp^8. For clarity, Phe^{175} is not shown. Water molecules are labeled *W*; the electron density is contoured at 2.25σ in *A* and *B* and at 2.0σ in *C* (this figure and Figs. 2, 4, and 6 were generated with BOBSCRIPT (44)). *FMT*, formate.

from 20.0 to 2.1 Å resolution. Refinement and model statistics are given in Table I. The enzyme structures complexed with MCPA and MCAA have an r.m.s. deviation of only 0.13 Å for all 490 Cα atoms, and consequently the results discussed below refer to both molecules unless stated otherwise.

Analysis of the Structures—The structures were analyzed using programs from the *CCP*4 suite (31), LSQMAN (32), VOIDOO (33), and the BIOMOL package (Protein Crystallography Group, University of Groningen). The atomic coordinates and structure factor amplitudes have been deposited in the Protein Data Bank with the entry codes 1qq5, 1qq7, and 1qq6 for MCPA (pH 8), MCPA (pH 5), and MCAA (pH 5) experiments, respectively.

RESULTS AND DISCUSSION

Native Structure at pH 8 and 1.52 Å Resolution—The structure of dimeric L-2-haloacid dehalogenase at pH 8 is very similar to the previously reported 1.95 Å resolution structure (8), with an r.m.s. difference of 0.47 Å for all 490 Cα atoms. This difference can be attributed to a few regions in the protein where the molecule has been modeled differently (see "Materials and Methods"). The disorder observed before in two loops and the C terminus (residues 25–27, 204–206, and 243–245) is present in this structure as well. The high resolution of the data enabled the identification of alternate conformations for 17 side chains. Moreover, in both molecules residues 208–213 were modeled in two different ways to account for ambiguities in the electron density. This region is part of the two-helix excursion (residues 193–219) that contributes significantly to the dimerization interface. Residues 208–213 in molecule A interact with the same residues in molecule B (Fig. 2). It is surprising to see that equally good dimerization contacts can be made by two different conformations.

The A and B molecules of the dimer can be superimposed with an r.m.s. difference of 0.29 Å for 245 Cα atoms. The major differences are found around the rebuilt residues (Pro^{107}, the loop from residues 204–207, and the C terminus). None of these differences are considered functionally relevant, and therefore all results discussed below pertain to both molecules, unless stated otherwise. The active site of the enzyme at pH 8 contains a formate ion that originates from the crystallization solution. This ion was observed in the 1.95 Å resolution structure as well, and its position was used to construct a model for the binding of an L-MCPA substrate (8). To replace the formate ion by MCPA, the crystal was washed several times. Apparently, the washing procedure was not sufficiently adequate to remove the ion.

Active Site Structure of the Enzyme-Ester Intermediates—In the experiments with MCPA and MCAA at pH 5, a substrate is covalently bound in the active site of DhlB. In these structures, it has replaced the formate ion and the water molecules that were present in the native structure. Very clearly, continuous electron density extends from the Asp^8 Oδ1 atom to the C_2 atom of the substrates, whereas no density for a covalently attached chlorine atom is observed (Fig. 1, *B* and *C*). This indicates that a covalent bond has formed between the nucleophilic Asp^8 residue and the substrate and that the covalent Cl–C bond in the substrate has been cleaved. The Asp^8 Oδ2 atom has a carbonyl functionality in the enzyme-ester intermediate structure. It is hydrogen-bonded to the hydroxyl group of the Thr^{12} side chain and the side chain amide group of Asn^{173} (Fig. 3*A*). Furthermore, in the MCPA covalent intermediate Ser^{171} Oγ is located within a 3.3-Å distance, but it is not in the plane of the carbonyl oxygen atom lone electron pairs. In the MCAA bound structure, however, the derivatized Asp^8 side chain is rotated −30° about the Cβ–Cγ bond, bringing Ser^{171} Oγ much closer to the Oδ2 atom and at the same time increasing the distance to Thr^{12} Oγ1 (Fig. 3*B*). This suggests a rotational freedom in the enzyme-ester intermediate, which might be used to optimize the interactions of the Oδ2 atom with the enzyme in the hydrolysis step of the reaction, when a negative charge develops on the Asp^8 Oδ2 atom. The negative charge of this oxyanion intermediate might be stabilized by Thr^{12}, Ser^{171}, and Asn^{173}, which together would form an oxyanion hole with a tetrahedral coordination of the oxyanion.

A chloride ion is present close to the substrate C_2 atom, Asn^{115}, and Arg^{39}. It is found in line with the Asp^8 Oδ1–C_2 bond, at a distance of 3.6 Å from the C_2 atom of the substrate, and the ion is close to both Nη atoms of Arg^{39} and to the side chain amide group of Asn^{115}. Both amino acid residues were shown to be catalytically essential in the L-DEX YL enzyme (1), but the chloride ion was not found in the covalent intermediate structures of this enzyme (12). Furthermore, the chloride is located in the plane of the aromatic ring of Phe^{175} at a closest distance of 4.7 and 4.2 Å in the MCPA and MCAA experiments, respectively. The difference is because of the interaction of the phenyl ring with the methyl group of the MCPA substrate, which is absent in MCAA. Aromatic ring systems are known to be partially positively charged in the plane of the ring (34) and binding interactions of tryptophan and tyrosine rings with halide ions have been observed before in haloalkane dehalogenase (DhlA) (35, 36). In 4-chlorobenzoyl-CoA dehalogenase the active site is surrounded by aromatic residues as well (37). Other aromatic residues near the DhlB active site, Tyr^{10} and Phe^{58}, have a less favorable ring orientation. The stabilizing cradle of positively charged and polar amino acids most likely

TABLE I
Statistics of data collection and quality of the final models

	Dh1B + MCPA, pH 8.0	Dh1B + MCPA, pH 5.0	Dh1B + MCAA, pH 5.0
Cell dimensions (Å)	a = 57.05, b = 83.93, c = 91.23	a = 56.75, b = 83.83, c = 90.81	a = 56.93, b = 83.56, c = 90.06
Resolution range (Å)	30–1.52	99–1.70	99–2.10
Highest resolution shell	(1.55–1.52)	(1.73–1.70)	(2.14–2.10)
Total no. of observations	306,585	202,654	276,852
No. of unique reflections	63,057	48,184	22,242
Completeness (%)[a]	92.7 (81.4)	99.0 (84.1)	87.2 (73.1)
$\langle I/\sigma(I)\rangle$	12.4 (2.2)	24.1 (7.0)	7.3 (3.2)
R_{merge} (%)	6.4 (35.1)	3.8 (14.5)	6.8 (22.1)
Quality of the final model			
No. of atoms	4,509	4,667	4,520
Protein[b]	3,932 (155)	4,000 (224)	3,994 (462)
Substrate/formate	6	10	8
Chloride		2	2
Solvent[b]	571 (8)	655 (9)	516 (9)
Final R-factor (%)	19.8 (20–1.52 Å, all data)	17.0 (20–1.70 Å, all data)	17.1 (20–2.10 Å, all data)
Free R-factor (%)	23.2 (20–1.52 Å, test set)	19.9 (20–1.70 Å, test set)	21.9 (20–2.10 Å, test set)
r.m.s.d. from ideality for			
Bond lengths (Å)	0.006	0.006	0.007
Bond angles (°)	1.1	1.1	1.1
Dihedrals (°)	21.4	21.5	21.4
ΔB for bonded atoms (Å^2)	1.6	1.1	1.0
$\langle B\rangle$ overall (Å^2)	25.4	23.7	23.2
$\langle B\rangle$ protein (Å^2)	22.8	22.5	21.5
Estimated coordinate error (Å)[c]	0.14; 0.18	0.09; 0.17	0.20; 0.16
Cross-validated estimated coordinate error (Å)[d]	0.18; 0.22	0.13; 0.20	0.27; 0.24

[a] Values in parentheses are for the highest resolution bin.
[b] Values in parentheses are the number of atoms in alternative conformations.
[c] Estimated from σ plot (18) and Luzzati plot (45), calculated from all data better than the 5.0 Å resolution.
[d] Estimated from cross-validated σ_A and Luzzati plots (46), calculated from test set data in the 5.0–1.52 Å resolution range.

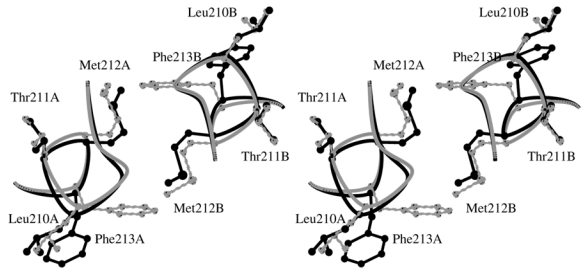

FIG. 2. **Two conformations of residues 208–213 of molecules A and B at the dimerization interface.**

functions to bind the halogen moiety of the substrate and to counterbalance the negative charge that develops on the halide during cleavage of the C–Cl bond.

The carboxylate moiety of the substrate is bound in the same position as the formate ion in the native DhlB structure. It is held in position by electrostatic interactions of its O_1 atom with the main chain NH groups of residues 9 and 10 and with the side chain of Ser^{114} (Fig. 3). The other carboxylate oxygen atom is hydrogen bonded to the main chain NH group of Asn^{115} and the Lys^{147} ϵ-amino group. The latter interaction is facilitated by a reorientation of the lysine side chain. In the native structure, the lysine is hydrogen-bonded to Asp^{176} Oδ2, the main chain carbonyl oxygen atom of residue 113, and Asp^8 Oδ1. The geometry of the contact with the formate ion is unfavorable for hydrogen bond formation. Because of the reorientation of Lys^{147} in the MCPA- and MCAA-bound structures, its interaction with Asp^8 Oδ1 has weakened. This is in accordance with the change of the functionality of the oxygen atom to an ether oxygen, which is generally a weaker hydrogen bond acceptor (38). All side chains that contribute to the binding of the carboxylate moiety were shown to be catalytically critical in L-DEX YL (1).

The structure of the complex with MCPA, the only chiral substrate to be efficiently degraded by DhlB (9), shows clear electron density for the C_3 atom of the substrate (Fig. 1*B*). The pocket in which the CH_3 group is located is not particularly hydrophobic as it is lined by side chain atoms of Lys^{147}, Asn^{173}, Phe^{175}, and Asp^{176}. It is shielded from the solvent by residues from helices α2 and α10, thereby limiting its size to about 75 Å^3. This explains why the substrate specificity of DhlB is restricted to small haloalkanoates (9). The position of the small pocket also resolves the preference of the enzyme for L-substrates; as for any substrate with the methyl group and the hydrogen atom interchanged at the C_2 position, steric clashes with main chain atoms of residues 10 and 11 would occur (Fig. 4*A*).

The overall structures of native DhlB and the reaction intermediates are very alike (see "Materials and Methods"), demonstrating that the native enzyme is in an active conformation. All DhlB structures represent a form of the enzyme in which the active site is very compact and shielded from the solvent. This is in contrast with L-DEX YL, in which a significant movement of the Asp^8-Ser^{18}, Tyr^{89}-Asp^{100}, and Leu^{113}-Arg^{131} regions toward the active site was observed in the structures of the covalent substrate complexes of L-DEX YL compared with the wild-type enzyme, which is more open (12). The compact form of DhlB could be caused by the extra two-helix subdomain that is not present in L-DEX YL and that in part closes off the entrance to the active site (8).

Li *et al.* (12, 13) have succeeded in trapping a covalent intermediate using L-2-monochloro-*n*-butyrate and the S171A mutant of L-DEX YL, which has an impaired oxyanion hole. Comparison of the DhlB and L-DEX YL covalent intermediate structures shows that the alkyl tail of the butyrate is close to the position of the chloride ion in DhlB (Fig. 4, *A* and *B*). In view of the 40% amino acid sequence identity between the two enzymes, one would expect that the catalytic residues and the

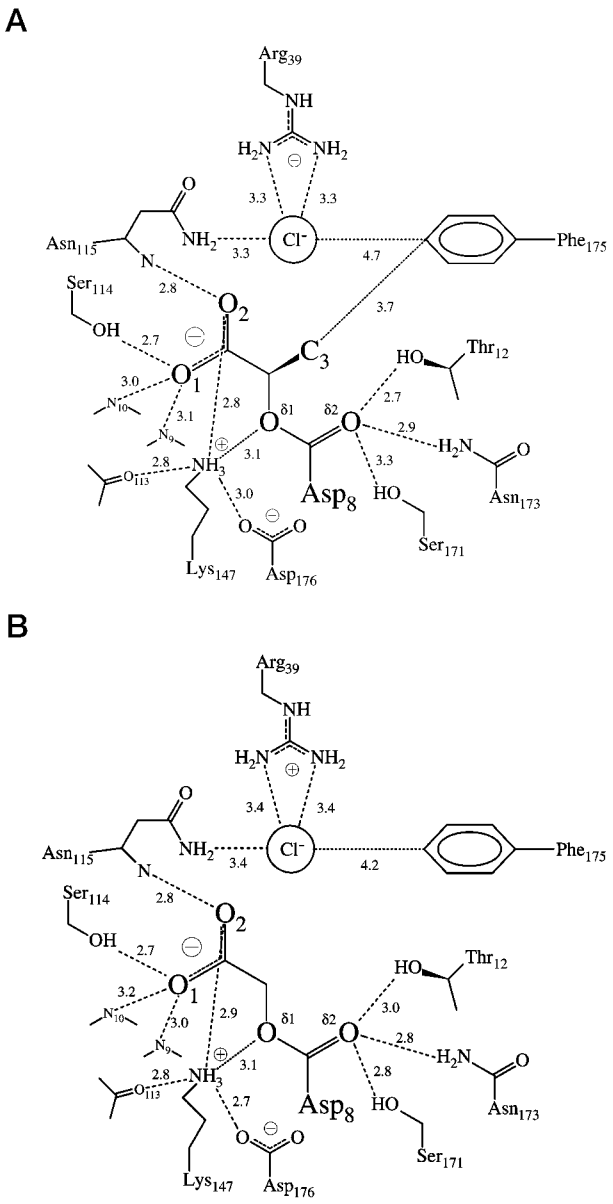

FIG. 3. **Schematic representation of the interactions in the covalent complexes of DhlB with L-2-monochloropropionate (*A*) and monochloroacetate (*B*).** Hydrogen bonding interactions with the covalent intermediate and the chloride ion are represented by *dashed lines*, and other interactions are represented by *dotted lines* with interatomic distances in Å.

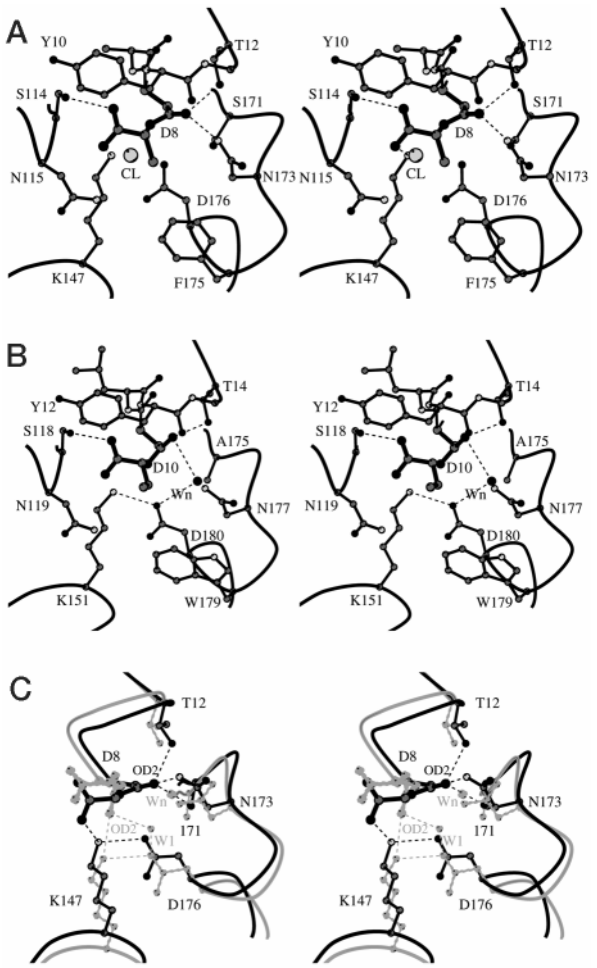

FIG. 4. **Stereo view of the covalent enzyme-ester intermediate with the chiral substrate L-MCPA, explaining the stereospecificity of the enzyme.** *A*, DhlB; *B*, structure of L-DEX YL with L-2-monochloro-*n*-butyrate bound; *C*, superimposition of MCAA-bound structures of DhlB and L-DEX YL.

residues that stabilize the Asp^8 Oδ2 oxyanion and the halide ion would be absolutely conserved. In DhlB, Asn^{173} is part of the oxyanion hole and Phe^{175} is involved in halide binding, and it is hard to imagine that the same residues in L-DEX YL would contribute only to the binding of the alkyl tail of the substrate as Li *et al*. (12) suggest. Another difference is found with the MCAA binding experiments. All DhlB structures and all but the MCAA-bound L-DEX YL structures are very similar with respect to the orientation of the Asp^8 side chain. The aberrant side chain conformation of Asp^8 in the MCAA-bound L-DEX YL structure is stabilized by hydrogen bonds of the Asp^8 Oδ1 ether oxygen atom to Thr^{12} and of the Asp^8 Oδ2 carbonyl oxygen atom to the Lys^{147} ϵ-amino group (Fig. 4*C*). This might be because of the L-DEX YL S171A mutation, which caused the loss of the attractive interaction between Asp^8 Oδ2 and Ser^{171} Oγ, present in the wild-type enzyme. Further research is required to establish whether the binding modes of the covalently bound complexes of L-DEX YL with MCAA and *n*-butyrate are of functional relevance.

Implications for the Reaction Mechanism—The dehalogenation reaction catalyzed by DhlB starts with the import of the negatively charged substrate via the cleft between the main domain and the four-helix bundle subdomain. The substrate can be either "pulled in" by an overall electrostatic dipole, which is directed along the dimer axis that is parallel to the import route (8), or via a guidance mechanism in which Arg^{39} plays a major role (12). The substrate is bound through specific binding interactions of its functional groups with conserved active site residues. The structures presented here demonstrate that the reaction proceeds through a nucleophilic attack of the Asp^8 Oδ1 atom on the C_2 of the substrate, resulting in the formation of a covalent enzyme-ester intermediate (Fig. 5). The salt bridge to the positively charged Lys^{147} side chain reduces the pK_a of the aspartate, thereby increasing its nucleophilicity. The formation of the Oδ1–C_2 bond is accompanied by the cleavage of the C_2–Cl bond. These three atoms are found in line, with the chloride ion located in a halide-stabilizing cradle formed by the side chains of Arg^{39}, Asn^{115}, and Phe^{175}. As a result, the configuration of the other three substituents of the C_2 atom is inverted, which is in agreement with the observed inversion of configuration at the chiral center of the substrate (9).

In the next step of the reaction, the ester bond is hydrolyzed by a nucleophilic attack of a water molecule (or hydroxyl ion) on

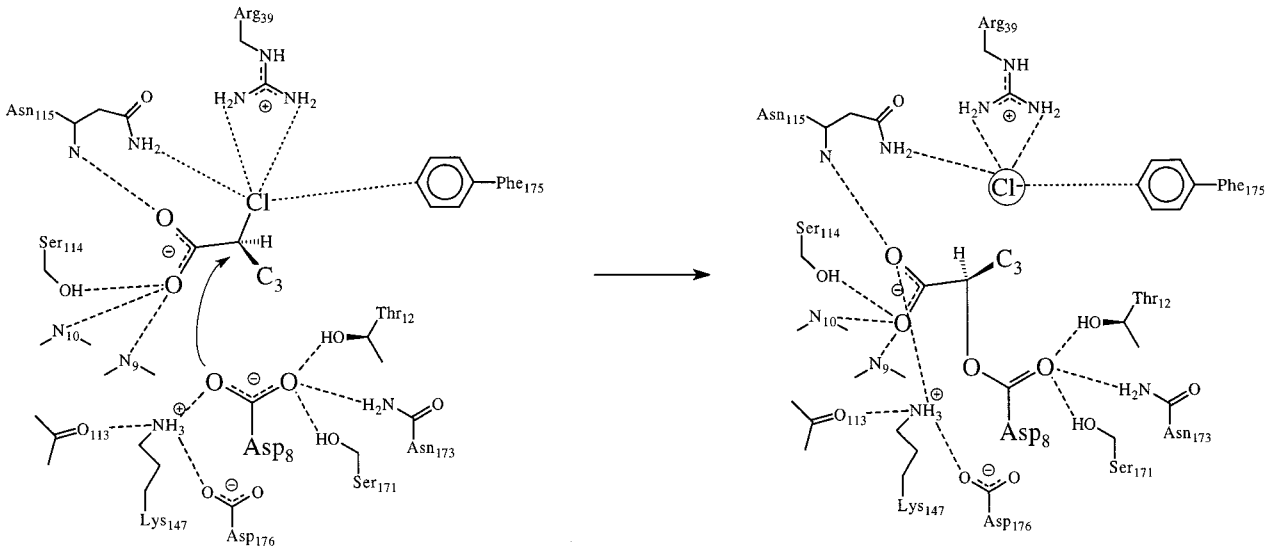

FIG. 5. **Reaction scheme for the proposed reaction of L-2-haloacid dehalogenase.**

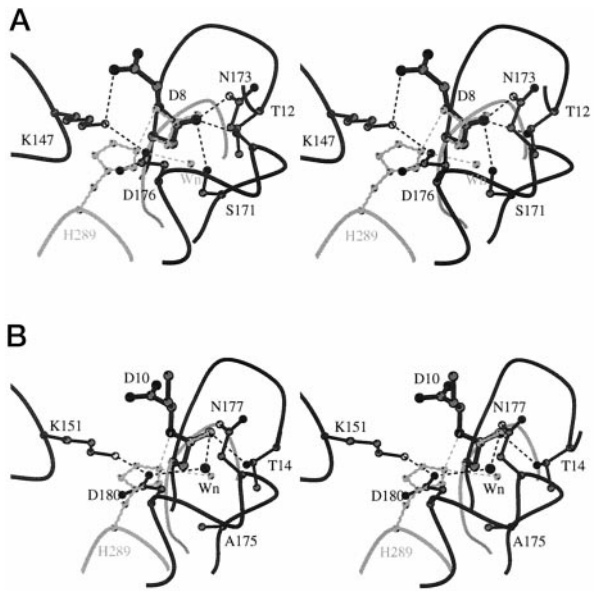

FIG. 6. **Stereo view of the superimposition of the active sites of the MCPA-DhlB complex and haloalkane dehalogenase (*A*) and of the L-2-monochloro-*n*-butyrate-L-DEX YL complex and haloalkane dehalogenase (*B*).** Only the Cα, Cβ, Cγ, Oδ1, and Oδ2 atoms of the nucleophilic aspartate residues were superimposed with r.m.s. differences for *A* and *B* of 0.19 and 0.09 Å, respectively. In *B*, the proposed L-DEX YL nucleophilic water molecule Wn is only 0.9 Å away from its DhlA counterpart.

the Cγ atom of Asp^8 (10). The negative charge, which develops on the Oδ2 carbonyl oxygen atom, is stabilized by an oxyanion hole formed by side chain atoms from Thr^{12}, Asn^{173}, and Ser^{171}. The nature of the hydrolytic water molecule and its activation is still subject to speculation, as there is no such molecule present within 6 Å from the Asp^8 Cγ atom in the DhlB covalent intermediates. A movement of a part of the enzyme would be required to allow a water molecule to enter the active site. In the S171A L-DEX YL mutant one water molecule (Wn) was found near the ester bond (12), but it occupies a position near where the Ser^{171} Oγ atom would be in the wild-type enzyme. However, the Asp^8 Cγ atom is accessible from this side only, as main chain atoms from residues 9–12 prohibit the approach of a water molecule from the other side (Fig. 4*A*). Lys^{147} and Asp^{176} are possible candidates to activate a water molecule that attacks the Asp^8 Cγ, as they are located close to the ester bond to be cleaved. The pK_a of a lysine side chain (~10) (39) is around the relatively high pH optimum of 9.5 for DhlB (9), but the different orientations of Lys^{147} in the various structures point at a flexibility of this side chain that could hamper directing a nucleophilic water molecule. Moreover, the two nearby negatively charged carboxylate moieties of the substrate and Asp^{176} might increase the pK_a of the residue.

A comparison of the esterified nucleophile of DhlB and its immediate environment with the covalent intermediate of DhlA (14) shows that the Nϵ2 atom of the His^{289}, the residue which activates the hydrolytic water molecule, takes up a position in between Lys^{147} Nζ and Asp^{176} Oδ2, although closer to the latter (Fig. 6). Furthermore, the position of the DhlA nucleophilic water molecule is then close to Asp^{176} Oδ1 and Ser^{171} Oγ and very near Wn in the L-2-monochloro-*n*-butyrate-L-DEX YL complex. This supports the suggestion from Li *et al.* (12) that Asp^{176} and Ser^{171} are essential for hydrolysis of the ester. Above pH 9, the enzyme could employ the flexibility of Lys^{147} to vacate the space needed for the water, driven by a pH effect. We have not been able to obtain stable crystals at pH 9 or higher, which is indicative of structural changes around this pH. Also the dimer interface might be susceptible to change around the pH optimum, as Lys^{41} and Tyr^{68} of both molecules make hydrogen bonds to the main chain carbonyl groups of Leu^{216} and Ala^{215}, respectively, and the donor groups are only 4 Å apart. Lys^{147} could also play a role in the deprotonation of Asp^{176} after hydrolysis, although Tyr^{153}, the other residue hydrogen bonded to Asp^{176}, is another candidate for this function.

Many of the residues in the active site are conserved among the members of the HAD superfamily (5, 6). The model, which was constructed for the structure and mechanism of the phosphatase and P-type ATPase members of the superfamily (40), is fully corroborated by the DhlB enzyme-ester intermediate structures. These enzymes cleave covalent bonds of phosphorylated substrates by nucleophilic attack of the motif I Asp (Asp^8) on the phosphorus of the substrate, resulting in the formation of a phosphoenzyme intermediate (41, 42). Like in DhlB, the motif II Ser/Thr (Ser^{114}) and the motif III Lys (Lys^{147}) partly compensate the negative charge of the intermediate. Two of the three residues of the oxyanion hole in L-DEXs, Ser^{171}, and Asn^{173} are not found in the phosphatase and P-type ATPase members of the superfamily. This is not surprising as the proposed hydrolytic mechanism does not include the formation of an oxyanion intermediate, but instead the phosphoenzyme intermediate is hydrolyzed by attack on the phos-

phorus atom (43). The negative charge that develops on the phosphoryl group was proposed to be counterbalanced by a magnesium ion (40).

Although many details of the L-DEX mechanism are now well understood, it is evident that further research is required to resolve the hydrolysis step of the dehalogenation mechanism of L-2-haloacid dehalogenase. In particular, a three-dimensional structure of the native enzyme at the pH optimum of 9.5 could provide useful information about the position of the nucleophilic water molecule, although so far we have not been able to obtain crystals that are stable at this pH.

Acknowledgments—It is a pleasure to acknowledge Dr. D. B. Janssen and co-workers for their supply of protein and useful comments. We thank Drs. K. S. Wilson, V. S. Lamzin, and other staff of the European Molecular Biology Laboratory Outstation, Deutches Electronen Synchrotron, Hamburg for access to the synchrotron data collection facilities and assistance. We thank the European Union for support of the work at the European Molecular Biology Laboratory, Hamburg through the Human Capital and Mobility Programme to Large Installations Project contract no. CHGE-CT93-0040. We gratefully acknowledge Dr. W. P. Burmeister and other staff of the ESRF, Grenoble for access to the synchrotron data collection facilities and assistance. We thank ESRF for support of the work at ESRF, Grenoble.

REFERENCES

1. Kurihara, T., Liu, J.-Q., Nardi-Dei, V., Koshikawa, H., Esaki, N., and Soda, K. (1995) *J. Biochem.* (*Tokyo*) **117,** 1317–1322
2. Janssen, D. B., Scheper, A., Dijkhuizen, L., and Witholt, B. (1985) *Appl. Environ. Microbiol.* **49,** 673–677
3. Fetzner, S. (1998) *Appl. Microbiol. Biotechnol.* **50,** 633–657
4. Stucki, G., and Thüer, M. (1995) *Environ. Sci. Technol.* **29,** 2339–2345
5. Koonin, E. V., and Tatusov, R. L. (1994) *J. Mol. Biol.* **244,** 125–132
6. Aravind, L., Galperin, M. Y., and Koonin, E. V. (1998) *Trends Biochem. Sci.* **23,** 127–129
7. Hisano, T., Hata, Y., Fujii, T., Liu, J.-Q., Kurihara, T., Esaki, N., and Soda, K. (1996) *J. Biol. Chem.* **271,** 20322–20330
8. Ridder, I. S., Rozeboom, H. J., Kalk, K. H., Janssen, D. B., and Dijkstra, B. W. (1997) *J. Biol. Chem.* **272,** 33015–33022
9. van der Ploeg, J., van Hall, G., and Janssen, D. B. (1991) *J. Bacteriol.* **173,** 7925–7933
10. Liu, J.-Q., Kurihara, T., Miyagi, M., Esaki, N., and Soda, K. (1995) *J. Biol. Chem.* **270,** 18309–18312
11. Liu, J.-Q., Kurihara, T., Miyagi, M., Tsunasawa, S., Nishihara, M., Esaki, N., and Soda, K. (1997) *J. Biol. Chem.* **272,** 3363–3368
12. Li, Y.-F., Hata, Y., Fujii, T., Hisano, T., Nishihara, M., Kurihara, T., and Esaki, N. (1998) *J. Biol. Chem.* **273,** 15035–15044
13. Li, Y.-F., Hata, Y., Fujii, T., Kurihara, T., and Esaki, N. (1998) *J. Biochem.* (*Tokyo*) **124,** 20–22
14. Verschueren, K. H. G., Seljée, F., Rozeboom, H. J., Kalk, K. H., and Dijkstra, B. W. (1993) *Nature* **363,** 693–698
15. Ridder, I. S., Rozeboom, H. J., Kingma, J., Janssen, D. B., and Dijkstra, B. W. (1995) *Protein Sci.* **4,** 2619–2620
16. Otwinowski, Z., and Minor, W. (1997) *Methods Enzymol.* **276,** 307–326
17. Navaza, J. (1994) *Acta Crystallogr. Sect. A Found. Crystallogr.* **43,** 157–163
18. Read, R. J. (1986) *Acta Crystallogr. Sect. A Found. Crystallogr.* **42,** 140–149
19. Bhat, T. N. (1988) *J. Appl. Crystallogr.* **21,** 279–281
20. Vellieux, F. M. D., and Dijkstra, B. W. (1997) *J. Appl. Crystallogr.* **30,** 396–399
21. Brünger, A. T. (1992) *Nature* **355,** 472–475
22. Rice, L. M., and Brünger, A. T. (1994) *Proteins Struct. Funct. Genet.* **19,** 277–290
23. Brünger, A. T., Adams, P. D., Clore, G. M., DeLano, W. L., Gros, P., Grosse-Kunstleve, R. W., Jiang, J.-S., Kuszewski, J., Nilges, M., Pannu, N. S., Read, R. J., Rice, L. M., Simonson, T., and Warren, G. L. (1998) *Acta Crystallogr. Sect. D Biol. Crystallogr.* **54,** 905–921
24. Engh, R. A., and Huber, R. (1991) *Acta Crystallogr. Sect. A Found. Crystallogr.* **47,** 392–400
25. MacArthur, M. W., and Thornton, J. M. (1996) *J. Mol. Biol.* **264,** 1180–1195
26. Ridder, I. S., Rozeboom, H. J., and Dijkstra, B. W. (1999) *Acta Crystallogr. Sect. D Biol. Crystallogr.* **55,** 1273–1290
27. Jones, T. A., Zou, J.-Y., Cowan, S. W., and Kjeldgaard, M. (1991) *Acta Crystallogr. Sect. A Found. Crystallogr.* **47,** 110–119
28. Laskowski, R. A., MacArthur, M. W., Moss, D. S., and Thornton, J. M. (1993) *J. Appl. Crystallogr.* **26,** 283–291
29. Hooft, R. W. W., Vriend, G., Sander, C., and Abola, E. E. (1996) *Nature* **381,** 272
30. Kleywegt, G. J., and Jones, T. A. (1997) *Methods Enzymol.* **277,** 208–230
31. Collaborative Computational Project No. 4 (1994) *Acta Crystallogr. Sect. D Biol. Crystallogr.* **50,** 760–763
32. Kleywegt, G. J., and Jones, T. A. (1997) *Methods Enzymol.* **277,** 525–545
33. Kleywegt, G. J., and Jones, T. A. (1994) *Acta Crystallogr. Sect. D Biol. Crystallogr.* **50,** 178–185
34. Burley, S. K., and Petsko, G. A. (1988) *Adv. Protein Chem.* **39,** 125–192
35. Verschueren, K. H. G., Kingma, J., Rozeboom, H. J., Kalk, K. H., Janssen, D. B., and Dijkstra, B. W. (1993) *Biochemistry* **32,** 9031–9037
36. Krooshof, G. H., Ridder, I. S., Tepper, A. W. J. W., Vos, G. J., Rozeboom, H. J., Kalk, K. H., Dijkstra, B. W., and Janssen, D. B. (1998) *Biochemistry* **37,** 15013–15023
37. Benning, M. M., Taylor, K. L., Liu, R.-Q., Yang, G., Xiang, H., Wesenberg, G., Dunaway-Mariano, D., and Holden, H. M. (1996) *Biochemistry* **35,** 8103–8109
38. Jeffrey, G. A., and Sänger, W. (1991) *Hydrogen Bonding in Biological Structures*, Springer-Verlag, New York
39. Fersht, A. R. (1985) *Enzyme Structure and Mechanism*, 2nd Ed., W. H. Freeman, New York
40. Ridder, I. S., and Dijkstra, B. W. (1999) *Biochem. J.* **339,** 223–226
41. Asano, S., Tega, Y., Konishi, K., Fujioka, M., and Takeguchi, N. (1996) *J. Biol. Chem.* **271,** 2740–2745
42. Collet, J.-F., Gerin, I., Rider, M. H., Veiga-da-Cunha, M., and van Schaftingen, E. (1997) *FEBS Lett.* **408,** 281–284
43. Dahms, A. S., Kanazawa, T., and Boyer, P. D. (1973) *J. Biol. Chem.* **248,** 6592–6595
44. Esnouf, R. M. (1997) *J. Mol. Graphics* **15,** 133–138
45. Luzzati, V. (1952) *Acta Crystallogr.* **5,** 802–810
46. Read, R. J. (1997) *Methods Enzymol.* **277,** 110–128